JOURNAL OF APPLIED ELECTROCHEMISTRY **27** (1997) 1313–1322

Flow visualization and modelling of a filter-press type electrochemical reactor

C. BENGOA*, A. MONTILLET, P. LEGENTILHOMME, J. LEGRAND

Laboratoire de Génie des Procédés, Institut Universitaire de Technologie, B.P. 420, 44606 Saint-Nazaire Cédex, France

Received 20 May 1996; revised 7 October 1996

A study of flow visualization and residence time distribution is provided in order to model the flow between two electrodes in a commercial filter-press reactor, the ElectroSynCell® from Electrocell AB. Flow visualization indicates that both axial and lateral dispersion phenomena occur and a global plug flow behaviour is observed. The flow distribution is asymmetric due to the design of the inlet system in the active zone. The flow throughout the cell is described by a dispersed plug flow model for which the mean residence time and the Péclet number are determined. The reaction area and the inlet system are separately analysed by locating conductimetric probes inside the electrochemical cell. The reaction area is also well described by a dispersed plug flow model, and characterized by high dispersion. The inlet system is, respectively, described by a dispersed plug flow model and by a cascade of continuous stirred tank reactors. The high number of reactors in the cascade denotes a quasi plug flow behaviour. The results are confirmed by two cascades of continuously stirred tank reactors in series. The dispersion coefficients obtained throughout the reaction area of the cell are not constant. This shows that the flow is not well established at the entrance of the reaction zone and depends on the entrance conditions.

List of symbols

D_{ax}	axial dispersion coefficient ($m^2 s^{-1}$)
d_c	depth of the channel (m)
d_e	hydraulic diameter of the channel (m)
E_r	mean root square error
$F(i\omega)$	transfer function in the Fourier domain
I	number of continuous stirred tank reactors in the first cascade
J	number of continuous stirred tank reactors in the second cascade
L	Length of the flow path in the reactor (m)
Pe	Péclet number, $Pe = U_0 L/\varepsilon D_{ax}$
Q_v	volumetric flow rate ($m^3 s^{-1}$)
Re	Reynolds number, $Re = d_e U_0/v$
$\bar{t}_s$	mean residence time (s)
U_0	mean superficial velocity ($m s^{-1}$)
w_c	width of the channel (m)
$X(t)$	experimental signal at the inlet of the studied section
$Y(t)$	experimental signal at the outlet of the studied section
$Y^*(t)$	calculated signal at the outlet of the studied section

Greek letters

ε	porosity
σ	standard deviation
v	kinematic viscosity ($m^2 s^{-1}$)
τ_1	mean residence time in the first cascade (s)
τ_2	mean residence time in the second cascade (s)

1. Introduction

In this paper, hydrodynamics of a commercially available filter-press type electrolyser, the ElectroSynCell® of Electrocell AB [1, 2], are studied. Previous papers [3, 4] have characterized the flow in the reactor working without a membrane, that is, with a single hydraulic circuit, in four representative unitary cells: a plane plate with a turbulence promoter, a plane plate with foams, a plane plate alone and, finally, a plane plate covered with a turbulence promoter and another one covered with a sheet of foam and forming a single channel. Also previously, the residence time distribution was determined using a voltammetric method with two measurement points.

The present work is dedicated to the local study and modelling of the flow between two electrodes, the first of which is covered with a turbulence promoter and the second with a sheet of foam. With this kind of configuration, the imbalance of the active surface areas of the two electrodes means that no membrane is required for some applications. First, the visualization of the reaction zone was studied by dye injection and electrode activated pH methods [3]. In

* Present address: Servei de Tecnologia Química, Escola Tècnica Superior d'Enginyeria, Universitat Rovira i Virgili, c/ Salou, s/n, 43006 Tarragona, Catalunya, Spain.

0021-891X

this case, four injection points were used to improve the visualization analysis. Secondly, two conductimetric cells were installed at the inlet and the outlet of the reactor so as to globally study the residence time distribution in the reactor. This should confirm the results obtained with the voltammetric method [4]. The reaction zone and the inlet–outlet (IO) system of the reactor were then modelled separately by locating conductimetric probes inside the reaction zone at the extremities of two plane plates simulating the electrodes. Finally, the local axial dispersion coefficients were determined using a set of four conductimetric probes distributed throughout the reaction zone of the electrochemical cell.

2. Experimental details

2.1. *Electrochemical cell*

The ElectroSynCell® electrolyser is commonly arranged by stacking representative unit cells made up of a plane plate, the electrode, which is covered by two 'inner' frames, consisting of plastic nets which act as turbulence promoters. The plastic net used is that especially designed by Electrocell AB for this electrolyser; it is a lattice of triangular polypropylene threads (Fig. 1) with a 10 mm × 8 mm diamond shaped mesh and a porosity of 0.90. The fluid distributor is located upstream of the reaction zone in the 'inner' frames. The 'inner' frames are inserted into a polymeric 'outer' frame. These representative unit cells have alternating anolyte and catholyte compartments, separated by membranes. An accurate description of the cell can be found elsewhere [4].

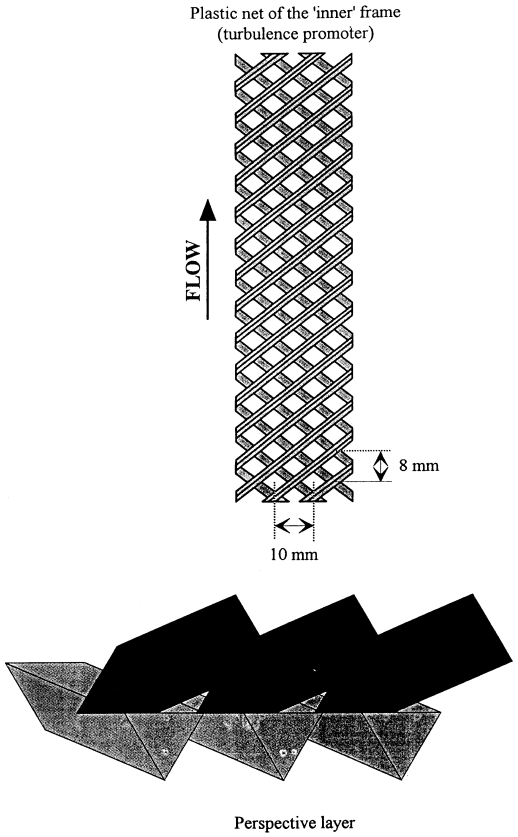

Fig. 1. Sketch of the turbulence promoter used in the ElectroSynCell®.

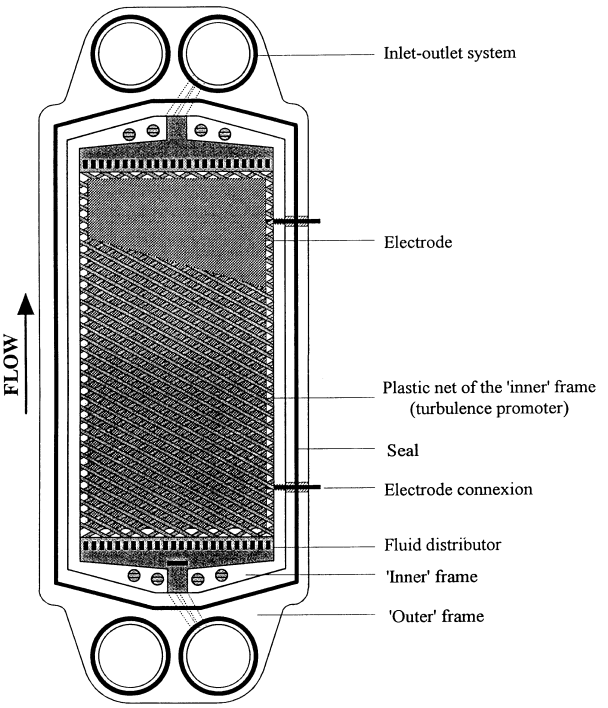

Fig. 2. Description of the different components of the ElectroSynCell®.

A diagram of the different components of the ElectroSynCell® is shown in Fig. 2. For the purpose of the experiments, no membrane is used between the electrodes, and a channel is defined as shown in Fig. 3, which restricts the flow in the area bordered by the 'inner' frames. Also, the plastic net of an 'inner' frame is removed and substituted by a sheet of foam of the same thickness (2.5 mm). The polyester open-cell foam used is grade 60 (pores per inch), with $2.5 \times 10^5\ m^{-1}$ surface area per volume of solid and a porosity of 0.975. Grade 60 is chosen because it offers a good compromise between the increase in surface area and the pressure drop [5]. In this configuration, the electrolyte flows along the channel formed by the two electrodes, which are 296 mm long (in the flow direction) and 140 mm wide, with an interelectrode gap of 5 mm. In the reaction zone, superficial velocity of the electrolyte in the channel, U_0, is varied between 3.0 and 24.6 $cm\ s^{-1}$. This geometry leads to a hydraulic diameter, d_e, of 9.66 mm. So, the Reynolds number, *Re*, based on this hydraulic diameter, and defined by

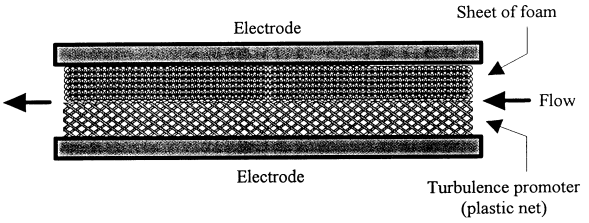

Fig. 3. Representative unit cell.

$$Re = \frac{d_e U_0}{v} = \frac{2U_0 w_c d_c}{(w_c + d_c)v} \quad (1)$$

lies between 300 and 2400. w_c and d_c are, respectively, the width and the depth of the channel, v being the kinematic viscosity of the working solution.

2.2. *Flow visualization*

Two specific techniques of direct flow visualization are used: dye injection and the electrode-activated pH method. The difference between the two methods is the kind of tracer injection or generation: a pulse being used in the former and a continuous one in the latter.

For the dye injection technique, bromocresol green ($0.4\,g\,dm^{-3}$) was used as an indicator. The tracer was injected at four points; three of these were located at the beginning of the active area and the last one upstream of the feed inlet system, as depicted in Fig. 4.

For the electrode activated pH method by anodic hydroxyl ion oxidation or cathodic hydroxyl ion reduction [6], thymol blue ($0.4\,g\,dm^{-3}$) was used as the analytical indicator and Na_2SO_4 (0.25 M) as the electrolyte. The working electrodes were stainless steel wires placed at the injection points located in the reaction zone. For each technique and injection point, six flow rates were tested: 75, 150, 225, 300, 375 and 450 $dm^3\,h^{-1}$. The flow in the reaction zone was filmed using a video camera, connected to a TV monitor and a video tape recorder. The video tape was further back-monitored in order to obtain instantaneous flow pictures.

For the purpose of this study, several modifications were made to the cell: one of the metallic frames and one of the electrodes were replaced by Plexiglas ones, so that the flow in the reaction zone was clearly seen. Figure 4 shows a schematic view of the experimental apparatus. No modification of the geometry and of the locations and design of the inlet and outlet systems were made with respect to the available commercial cell [1].

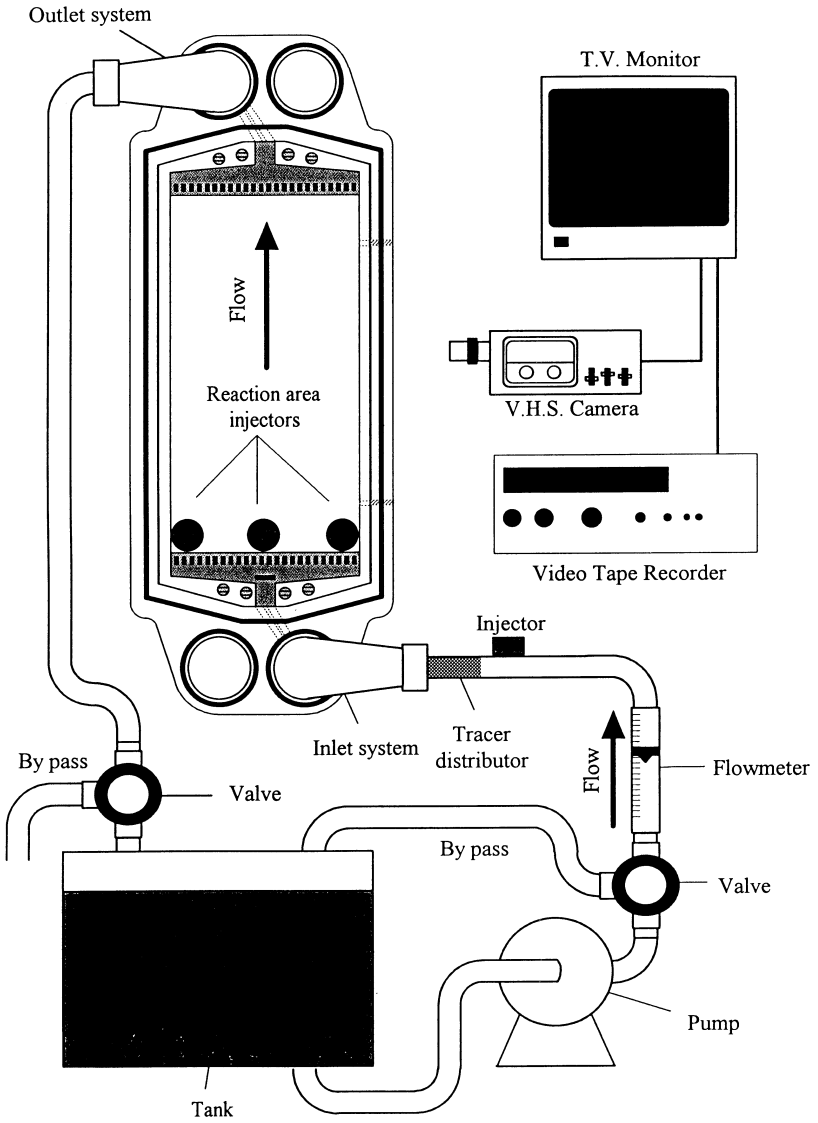

Fig. 4. Scheme of the experimental apparatus used during the visualization studies.

2.3. *Residence time distribution*

The residence time distribution (RTD) was experimentally determined with a conductimetric method with two measurement points [7]. To perform a global study, the concentration of the injected tracer (aqueous solution of sodium hydroxide) was measured, as a function of time, with two conductimetric cells located at the inlet and the outlet of the electrochemical reactor, respectively. The conductimetric cells consisted of two hemicylindrical plates insulated from each other. The cells were connected to two Tacussel CD810 variable frequency conductimeters. An operating frequency of 1000 Hz was adopted in order to avoid polarization of the electrodes and to ensure a linear relationship between the conductivity and the tracer concentration. Both concentration signals, obtained at the inlet and at the outlet of the cell, respectively, were sampled using an AOIP model SA32 data acquisition device, connected to a personal computer. Figure 5 shows a sketch of the equipment used in the global study. The hydraulic circuit was the same as that used in the visualization study, but the liquid was not recycled during the RTD experiments. The flow rates were incremented by steps of 20 dm^3h^{-1} between 100 and 620 $dm^3\,h^{-1}$.

In the reaction zone, RTD curves were experimentally determined using a set of four probes, distributed throughout the reaction zone of the electrochemical cell. Each probe consisted of two nickel strips, 140 mm × 5 mm, inserted in two Plexiglas plane plates replacing the original metallic electrodes. The distances between the conductimetric probes were 50, 136 and 271 mm, respectively, with respect to the leading edge of the plates (Fig. 6). The nickel conductimetric electrodes were designed in such a way that they covered the entire width of the reaction area. These nickel strips were periodically activated by successive generation of hydrogen and oxygen at their surfaces.

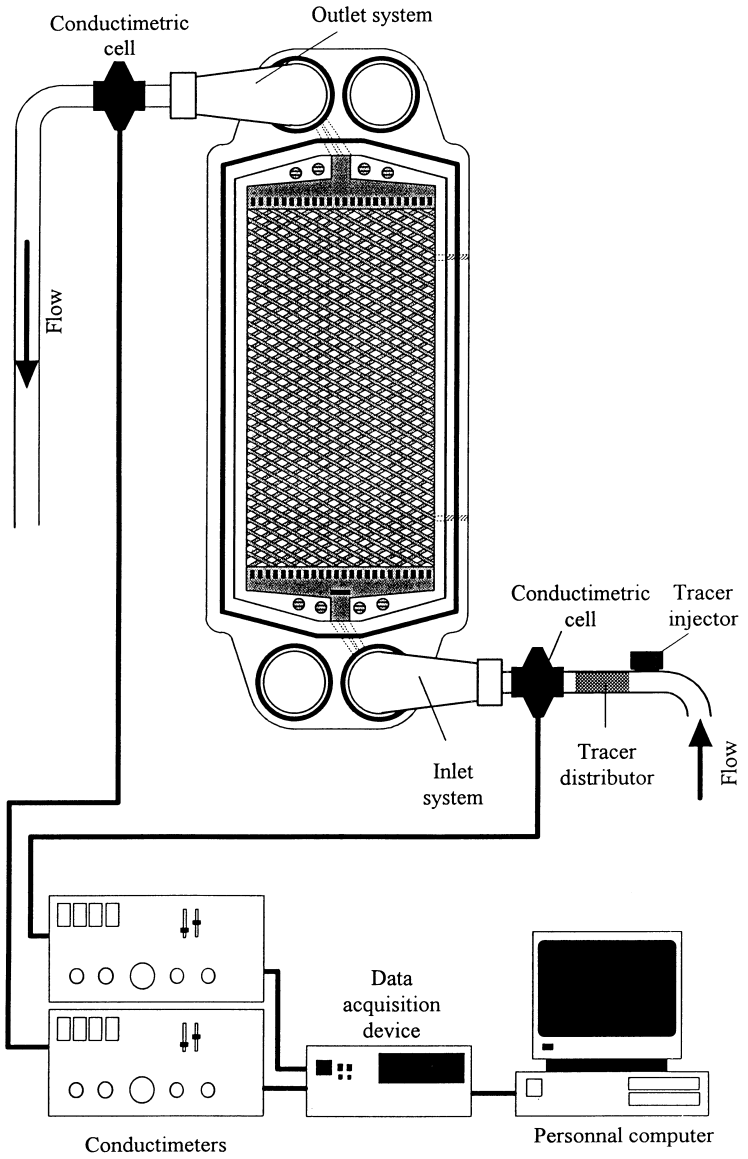

Fig. 5. Scheme of the experimental apparatus used during the residence time distribution studies.

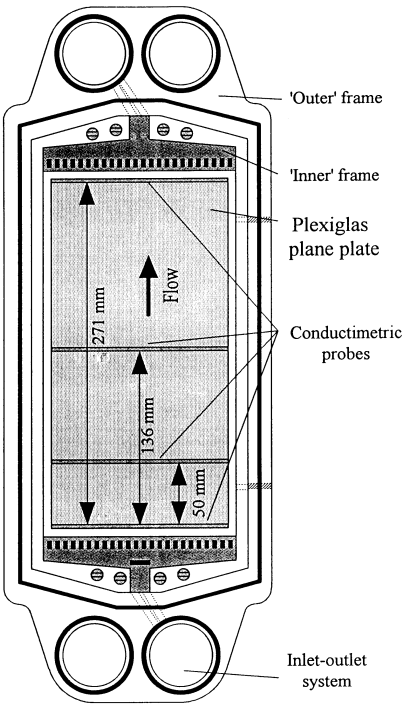

Fig. 6. Scheme of the modified electrode used during the local residence time distribution studies.

3. Flow visualization results

Figure 7, in which the results of the dye injection method are plotted, show both lateral and axial dispersion. In this configuration, the injected dye does not follow the rods of the acting net, as observed elsewhere [3, 8]. In this former work, the channels under study were filled with an acting net only (no foam was used) and a membrane partition configuration was adopted. In the present work, the absence of membrane partition and the use of a channel filled with a combination plastic net foam (Fig. 3) cause deviation from the typical flow pattern through a net. On the other hand, the flow does not correspond to plug behaviour in the reaction area. The flow pattern visualized is slightly asymmetric, the dye trace tends to drift to the left of the cell. This phenomenon may be explained by a small variation in the thickness of the channel. This behaviour is confirmed using the injection systems located on the right, where greater lateral dispersion is observed. Finally, dye injection before the inlet system shows that a nearly plug flow behaviour occurs at the entrance of the reaction zone (Fig. 8). The flow pattern is uniform along the reaction area. This behaviour is not caused by the reaction area itself, but by the inlet system that gives a plug character to the flow.

Globally, the flow configuration with a channel filled with a turbulence promoter and a sheet of foam appears intermediate between that observed with a turbulence promoter and that of the channel filled with a sheet of foam [3].

With the electrode activated pH method similar observations were made. Both lateral and axial dispersion are observed (Fig. 9).

4. RTD and modelling of the electrochemical cell

To enable a better understanding of the Sections following, the different flow models described below are schematically presented in Fig. 10.

4.1. *Modelling of the experimental curves*

By assuming that lateral dispersion is negligible with respect to longitudinal dispersion, and without chemical reaction, the concentration of the injected tracer is given as a function of time, t, and axial position, z, by the axial dispersed plug flow model:

$$\frac{\partial C}{\partial t} = D_{\mathrm{ax}} \frac{\partial^2 C}{\partial x^2} - \frac{U_0}{\varepsilon} \frac{\partial C}{\partial x} \tag{2}$$

The inlet, $X(t)$, and outlet, $Y(t)$, concentration curves are analysed by curve fitting in the time domain [9–11]. This method is considered to be the best way to determine the parameters of the model under study [9].

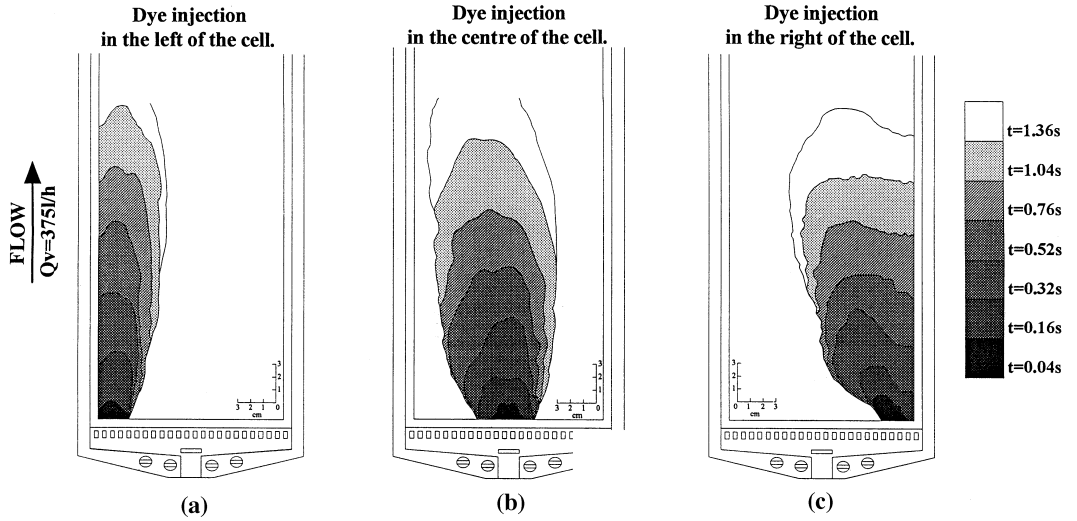

Fig. 7. Dye injection respectively in the left (a), the centre (b) and the right (c) of the cell.

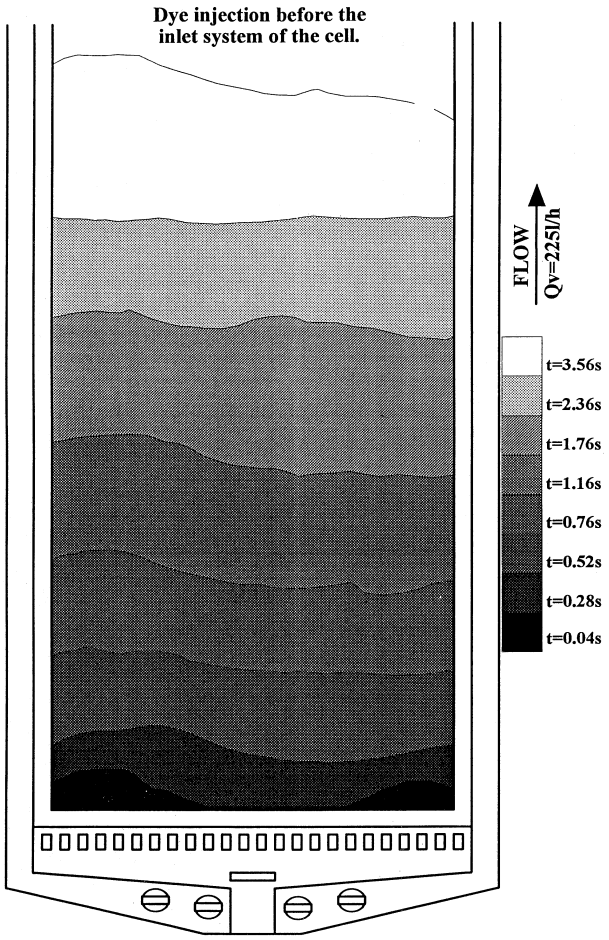

Fig. 8. Dye injection before the inlet system of the cell.

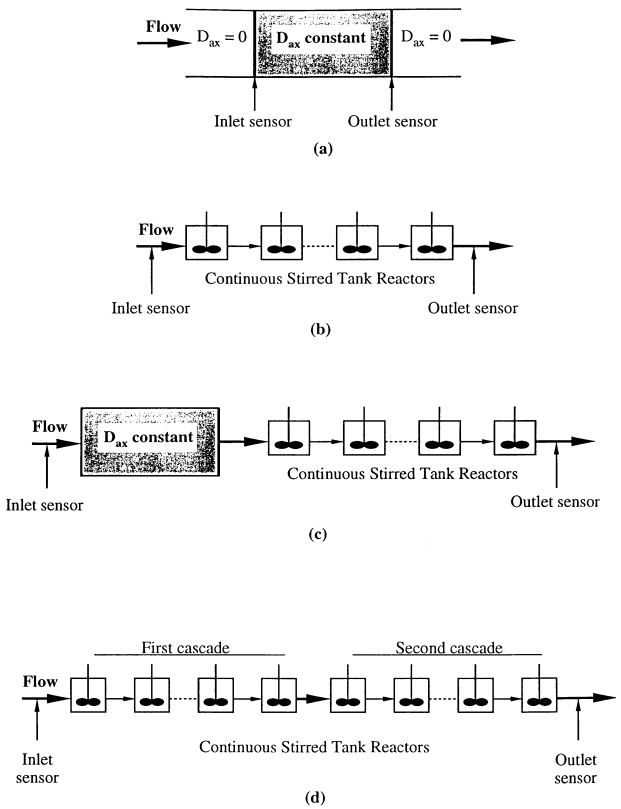

Fig. 10. Sketch of the different flow models tested in this work: (a) dispersed plug flow model (DPF); (b) cascade of identical volume continuous stirred tank reactors (CSTR); (c) dispersed plug flow model in series with a cascade of identical volume continuous stirred tank reactors (DPFCSTR); (d) two cascades of identical volume continuous stirred tank reactors (TCSTR)

Fahim and Wakao [9] have made a comparative study of the different methods of parameter estimation available in the literature (moment method, weighted moment method, Fourier analysis and time domain fitting) from measurements of tracer input and response signals; they found that curve fitting in the time domain gives more reliable values of the axial dispersion coefficients in packed beds. The experimental response (outlet curve) is compared with the calculated one, $Y^*(t)$, using the inlet curve and the transfer function of the model, $F(i,\omega)$, given by

$$F(i\omega) = \frac{\int_0^{2T} \exp(-i\omega) Y^*(t)\mathrm{d}t}{\int_0^{2T} \exp(-i\omega) X(t)\mathrm{d}t} \qquad (3)$$

The parameters of the model are optimized by minimizing the root mean square error, E_r, between

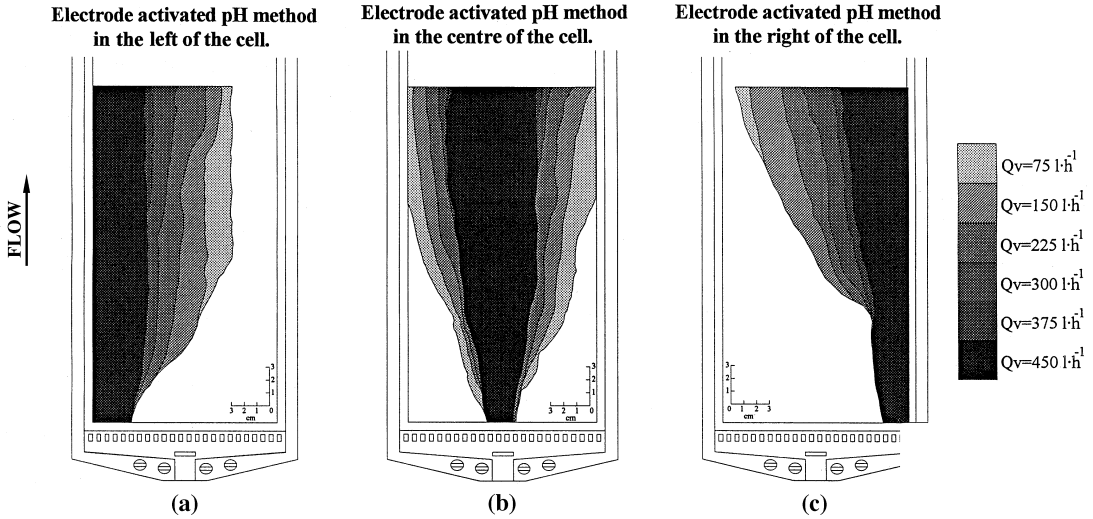

Fig. 9. Visualization by electrode activated pH method in the left (a), the centre (b) and the right (c) of the cell.

the calculated and experimental outlet signals using the Rosenbroock algorithm [12]:

$$E_r = \left[\frac{\int_0^{2T} \left(Y(t) - Y^*(t) \right)^2 dt}{\int_0^{2T} \left(Y(t) \right)^2 dt} \right]^{\frac{1}{2}} \quad (4)$$

where $2T$ is the time allowing the tail of the response signal $Y(t)$ to vanish.

4.2. *Global modelling of the electrochemical cell*

The dispersed plug flow (DPF) model was used to describe the global behaviour of the cell (Fig. 10 (a)). This model has been extensively used to describe the flow in reactors filled with porous media [3, 7, 13]. Its main advantage consists in its simple use for mass transfer and reactor performance calculations in packed reactors. The transfer function of the DPF model in the Fourier domain is given by [10]

$$F(i\omega) = \exp\left\{ \frac{Pe}{2} \left[1 - \left(1 + \frac{4}{Pe} \bar{t}_s \, i\omega \right)^{\frac{1}{2}} \right] \right\} \quad (5)$$

where the Péclet number, Pe, is defined by

$$Pe = \frac{U_0}{\varepsilon} \frac{L}{D_{ax}} \quad (6)$$

and U_0, ε and L are, respectively, the superficial velocity, the void fraction of the cell and the length of the cell. The Péclet number and the mean residence time, $\bar{t}_s$, are the two optimized parameters of the DPF model.

The experimental values of Pe are plotted against the volumetric flow rate Q_v in Fig. 11. The tested range is very similar to that previously studied by visualization and includes the hydrodynamic domain of the industrial cell. The value of the observed error, E_r, ranges between 3 and 5%, demonstrating that the DPF model is appropriate. The mean value of Pe and its corresponding standard deviation is 37.4 ± 2.2. These values are of the same order of magnitude as those presented by Montillet *et al.* [4].

However, for the commercially available cell the assembly of the plates simulating the electrodes is never exactly reproducible, so that the gap between these two plates is not absolutely constant within the reaction zone. On the other hand, the different nature of the materials may cause the flow to be perturbed. The high values of Pe observed confirm the visualization results, where the tracer concentration profile is uniform (Fig. 8), illustrating a quasi plug flow reactor.

4.3. *Reaction zone modelling*

The global modelling cannot explain the real behaviour of the flow in the reaction zone of the cell. In order to attempt to correctly model this zone, two probes were located at the ends of the plates, delimiting the reaction zone. First, a DPF model was used. The experimental values of the Péclet number are plotted against the volumetric flow rate, Q_v, in Fig. 12. The results show a uniform increase of the Péclet number with the flow rate. Dispersion is more important in the reaction zone.

This behaviour has been confirmed by flow modelling with a cascade of identical volume continuous stirred tank reactors (CSTR, Fig. 10 (b)). The transfer function of a CSTR in the Fourier domain is given by

$$F(i\omega) = \frac{1}{(1 + \tau_1 \, i\omega)^I} \quad (7)$$

where the mean residence time, τ_1, and the number of reactors, I, are optimized. The experimental results give a mean value of I between 3 and 5.

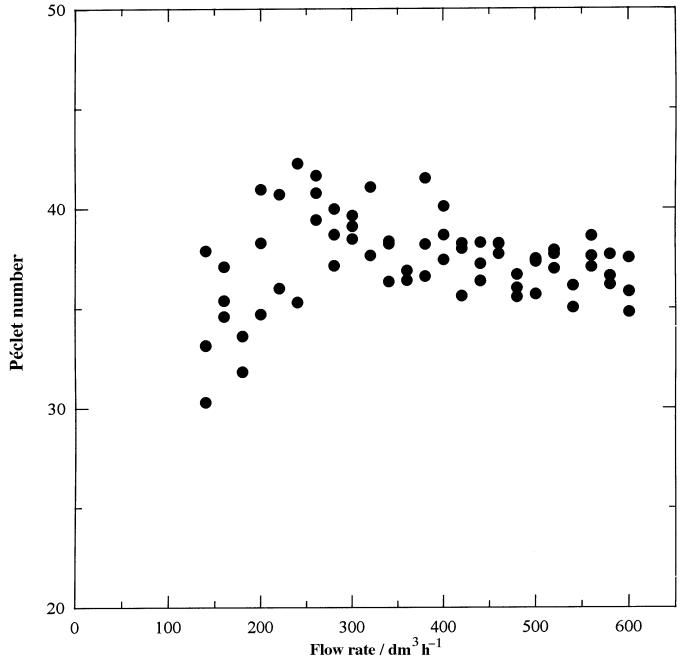

Fig. 11. Plot of Péclet number, Pe, against volumetric flow rate, Q_v, for the whole cell.

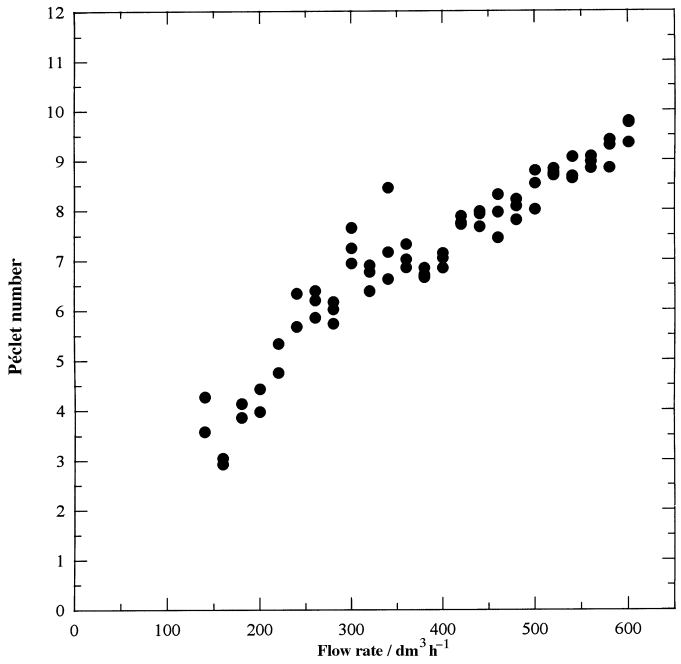

Fig. 12. Plot of Péclet number, Pe, against volumetric flow rate, Q_v, for the reaction area.

4.4. *Inlet–outlet system modelling*

Because of the geometrical structure of the I/O system, it was impossible to locate two identical conductimetric probes at each end of the system, and to directly measure the conductivity. To overcome this problem, we attempted to model the I/O system from the global model of the electrochemical cell and from the reaction zone model. For this goal, the whole electrochemical cell is described with a series (DPF-CSTR, Fig. 10 (c)) of a DPF model and a cascade of identical volume CSTR in series instead of a single DPF model (Section 4.2). The DPF corresponds to the flow in the reaction area and the CSTR to the flow in the I/O system. The transfer function of DPFCSTR in the Fourier domain is given by

$$F(i\omega) = \exp\left\{\frac{Pe}{2}\left(1 - \left(1 + \frac{4}{Pe}\bar{t}_s\, i\omega\right)^{\frac{1}{2}}\right)\right\} \times \frac{1}{(1 + \tau_2\, i\omega)^J} \qquad (8)$$

The parameters Pe and $\bar{t}_s$, corresponding to the reaction area, are fixed to the values obtained during the local study. The optimized parameters, corresponding to the I/O system, are τ_2 and J. The experimental modelling gives a mean value of J and its standard deviation as about 21 ± 4 reactors in the cascade, for the I/O system.

Finally, two cascades of identical volume CSTR in series (TCSTR, Fig. 10 (d)) were used to confirm the above results, the transfer function of TCSTR in the Fourier domain being

$$F(i\omega) = \frac{1}{(1 + \tau_1\, i\omega)^I} \times \frac{1}{(1 + \tau_2\, i\omega)^J} \qquad (9)$$

where τ_1 and I are the parameters corresponding to the reaction area and τ_2 and J are the parameters corresponding to the I/O system. τ_1 and I are fixed to the values obtained in the second modelling of the reaction zone (Section 4.3). The mean value of J and its standard deviation is 27 ± 4. This range of J values overlaps the preceding one, and confirms that the I/O system has a higher plug flow character. This behaviour agrees to a great extent with the visualization study.

4.5. *Local study of the reaction zone*

The final part of this work was devoted to the determination of the local axial dispersion coefficients within the active part of the cell. The DPF model was used to describe the different sections delimited by the conductimetric probes located in the reaction area, 50, 136 and 271 mm, respectively (Fig. 6). The experimental values of the Péclet number are plotted against the volumetric flow rate, Q_v, in Fig. 13. The mean values of the Péclet number and its corresponding standard deviations are 3.5 ± 0.7, 4.9 ± 1.4 and 7.2 ± 1.6 for lengths of 50, 136 and 271 mm, from the entrance of the active zone, respectively. To give a more precise overview of the problem, Fig. 14 shows the experimental values of the axial dispersion coefficients divided by the kinematic viscosity of the liquid, D_{ax}/v, against the Reynolds number, Re. This plot is more explicit because D_{ax}/v is a dimensionless parameter, which does not depend on the velocity and the length between the electrodes. For every experiment, D_{ax} increases with Re. But, it should be pointed out that the axial dispersion coefficient is not constant throughout the reaction area, it increases with the length between the probes. The difference

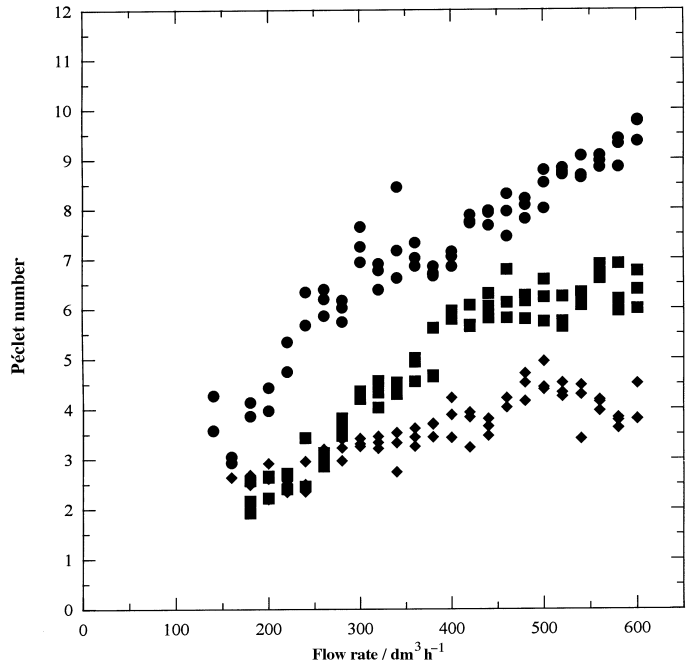

Fig. 13. Plot of Péclet number, Pe, against volumetric flow rate, Q_v, for the different distances in the reaction area. Electrode distances: (●) 271, (■) 136 and (◆) 50 mm.

between D_{ax} values denotes that the flow is not established in the reaction zone. This can be explained by the presence of turbulence at the beginning of the reaction area in the fluid inlet ($Re > 16000$). At the entrance section, the plane velocity profile caused by the turbulent flow regime progressively changes into a laminar-type flow in the reaction area. This laminar flow regime is confirmed by the increase in the axial dispersion coefficient. The progressive appearance of a laminar flow regime may induce a decrease in the value of the local mass transfer coefficient throughout the reaction area. A slight variation of the local mass transfer coefficient was observed by Brown *et al.* [14] in another commercial filter-press cell: the FM01-LC from ICI. On the other side, the proposed models may be used to predict the performance of electrochemical filter-press cells if electrochemical kinetics are known.

The mean values of the Péclet number and the number of reactors for each model are summarized in Table 1.

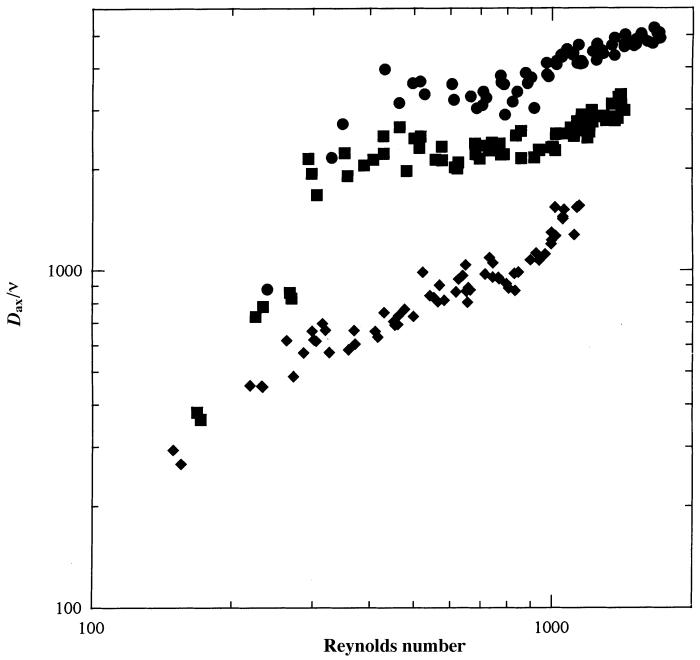

Fig. 14. Plot of the axial dispersion coefficient, D_{ax}, against the Reynolds number, Re, for the different distances in the reaction area. Electrode distances: (●) 271, (■) 136 and (◆) 50 mm.

Table 1. Mean values of the Péclet number and number of reactors for each model

Zone modelling	*Model*	*Result*
Global	DPF	No. of $Pe = 37.4 \pm 2.2$
Reaction	DPF	No. of $Pe = 7.2 \pm 1.7$
Reaction	CSTR	No. of reactors $= 4 \pm 1$
Inlet–outlet	DPFCSTR	No. of reactors $= 21 \pm 4$
Inlet–outlet	TCSTR	No. of reactors $= 27 \pm 4$

5. Conclusions

The flow visualization study of the configuration of the channel filled with a turbulence promoter and a sheet of foam demonstrated some important characteristics. Axial and lateral dispersion occurs in the reaction area. The dispersion asymmetry is the consequence of the asymmetrical distribution of the flow at the entrance to the reaction area. The inlet–outlet system gives the flow, and consequently the whole cell, a quasiplug flow character.

The flow throughout the cell is described by a DPF model, with high Péclet numbers (37.4 ± 2.2), and confirms the conclusions of the visualization study. The reaction area is also well described by a DPF model, with lower Péclet numbers (Fig. 12). These numbers are characteristic of relatively high dispersion and consequently of a low plug flow character. The results are confirmed by a model with a cascade of CSTR in series, with a very low number of reactors in the cascade (4 ± 1).

The inlet–outlet system was studied using a DPFCSTR model for the whole electrochemical cell, where the inlet-outlet system is described by the CSTR series. The number of reactors in this cascade simulating the inlet-outlet system (21 ± 4), is greater than that in the reaction area, and gives a quasiplug behaviour to the flow in the I/O system. These values are confirmed by the TCSTR model, where the number of reactors in the cascade relative to the I/O system is very similar (27 ± 4). All the results are in agreement with the visualization studies.

The calculation of the dispersion coefficients throughout the reaction area of the cell has demonstrated that the dispersion coefficient is not constant along the reactive zone. This shows that the flow is not well established in and throughout the reaction zone.

Acknowledgements

C.B. thanks the Direcció General de Recerca of Generalitat de Catalunya for financially supporting this research. The authors thank the Direction des Etudes et Recherches d'Electricité de France for supplying the ElectroSynCell®

References

[1] Electrocell AB, PO Box 34, S 18400, Akesberga, Sweden.
[2] L. Carlsson, B. Sandegren, D. Simonsson and M. Rihovsky, *J. Electrochem. Soc.* **130** (1983) 342.
[3] A. Montillet, J. Legrand, J. Comiti, M. M. Letord and J. M. Jud, 'Electrochemical Engineering and Energy', Plenum Press (1994), p.81.
[4] A. Montillet, J. Comiti and J. Legrand, *J. Appl. Electrochem.* **23** (1993) 1045.
[5] A. Montillet, PhD. thesis, Université de Nantes, Ecole Centrale de Nantes, France (1992).
[6] J. H. Gerard, *J. Fluid. Mech.* **46** (1971) 43.
[7] P. Legentilhomme, J. Legrand and J. Comiti, *J. Appl. Electrochem.* **19** (1989) 263.
[8] P. Feron and G. S. Solt, *Desalination* **84** (1991) 137.
[9] M. A. Fahim and N. Wakao, *Chem. Eng. J.* **25** (1982) 1.
[10] N. Wakao and S. Kaguei, 'Heat transfer in packed beds', Gordon & Breach, New York (1992).
[11] W. C. Clements, *Chem. Eng. Soc.* **24** (1992) 957.
[12] G. S. G. Beveridge and R. S. Schechter, 'Optimization: Theory and Practice', McGraw-Hill, New York (1992).
[13] P. Trinidad and F. C. Walsh, *Electrochim. Acta* **41** (1996) 493.
[14] C. J. Brown, D. Pletcher, F. C. Walsh, J. K. Hammond and D. Robinson, *J. Appl. Electrochem.* **22** (1992) 613.